Received: 24 January 2025 | Revised: 18 July 2025 | Accepted: 6 August 2025

DOI: 10.1002/VIW.20250015

VIEW

RESEARCH ARTICLE

Fungal DNA-barcoding on a chip: Magnetoresistive biosensors for yeast infection diagnosis

Maria Zolotareva[1,2,3] | **Francisco Cascalheira**[1,2] | **Rúben Afonso**[1] | **Maria Corado**[1] | **Ana Martins**[1] | **Cátia Caneiras**[4,5,6] | **Cristina Bárbara**[7,8] | **Miguel Cacho Teixeira**[2,9] | **Diogo Miguel Caetano**[1,3,10]

[1]Instituto de Engenharia de Sistemas e Computadores–Microsistemas e Nanotecnologias, INESC-MN), Lisbon, Portugal

[2]Institute for Bioengineering and Biosciences (iBB), Associate Laboratory Institute for Health and Bioeconomy–i4HB, Lisboa, Portugal

[3]Flash-Rapid Diagnostics Lda, Lisbon, Portugal

[4]Microbiology Research Laboratory on Environmental Health Institute of Environmental Health (ISAMB), Associate Laboratory TERRA, Faculty of Medicine, Universidade de Lisboa, Lisboa, Portugal

[5]Egas Moniz Center for Interdisciplinary Research, Egas Moniz School of Health and Science, Almada, Portugal

[6]Institute of Preventive Medicine and Public Health, Universidade de Lisboa, Lisboa, Portugal

[7]Institute of Environmental Health (ISAMB), Associate Laboratory TERRA, Faculty of Medicine, Universidade de Lisboa, Lisboa, Portugal

[8]Pulmonology Department, Unidade Local de Saúde Santa Maria, Lisboa, Portugal

[9]Department of Bioengineering, Instituto Superior Técnico, University of Lisbon, Lisboa, Portugal

[10]Department of Electrical and Computer Engineering, Instituto Superior Técnico, University of Lisbon, Lisboa, Portugal

Correspondence
Miguel Cacho Teixeira and Diogo Miguel Caetano
Email: mnpct@tecnico.ulisboa.pt and diogo.caetano@inesc-mn.pt

Funding information
FCT Fundação para a Ciência e a Tecnologia, Grant/Award Numbers: UIDB/04565/2020, UIDP/04565/2020, LA/P/0140/2020, UIDB/05367/2020, UIDP/05367/2020; NextGenerationEU, Grant/Award Number: HfPT–Health from Portugal; EIT Health Innovation Call, Grant/Award Number: Bactometer–RIS_innovation-068; MORE4MEDICAL, Grant/Award Number: ECSEL/0007/2019; HORIZON-KDT-JU-2023-1-IA, Grant/Award Number: 10.3030/101140192; OSCARS – Open Science Clusters' Action for Research and Society - Project FAIRY, Grant/Award Number: 101131096

Abstract

The worldwide burden of fungal infection has been increasing due to the expansion of the endemic borders, the host range of certain mycosis, and the emergence of novel opportunistic, drug and multi-drug-resistant fungal pathogens. Many deaths can be attributed to slow, inaccurate, or absent diagnostic testing and a lack of timely administration of effective antifungal treatment. Panfungal PCR followed by sequence identification has the practical advantage of rapidly and accurately detecting slow-growing, unculturable and even rare, unexpected or novel pathogens. We have developed and tested a robust and flexible biosensing diagnostic strategy, consisting of panfungal rDNA amplification, DNA hybridization, and magnetic labeling on a portable microfluidic setup. We designed DNA-capture probes specific for *Candida albicans*, *Candida auris*, *Nakaseomyces glabratus*, and *Cryptococcus neoformans*, and evaluated them for diagnostic sensitivity and specificity assessment, first in silico against a dataset of 58 pathogenic species (1239 DNA sequences), and then in vitro against the four species and 30 unsequenced clinical isolates of *N. glabratus*.

On-chip, our assay performed with 95% accuracy, 91% sensitivity, and 98% specificity under a limit of detection of 600 single-stranded amplified ITS DNA sequences. Our results demonstrate the diagnostic value of DNA-barcoding and magnetoresistive biosensing, emphasizing the revolutionizing potential of DNA-sequence-based technologies in clinical practice.

KEYWORDS
DNA biosensors, fungal infection diagnosis, hybridization probes, ITS probes, magnetic DNA labeling, molecular diagnostics

1 | INTRODUCTION

Pathogenic fungi are estimated to affect over a billion people annually, taking over 3.5 million lives,[1] while irreversibly compromising many others.[2,3] The incidence of fungal disease appears to be increasing, accompanied by epidemiological shifts,[4,5] and growing heterogeneity of infecting species.[6] Faced with an emerging crisis, the available diagnostic and treatment arsenal remains far insufficient. The lack of routine testing is justified by the low sensitivity, specificity, and availability of current diagnostic methods. Additionally, according to autopsy reports, invasive fungal infection has an estimated chance of being diagnosed before death of only 50%.[7]

Fungal pathogen identification is highly informative in guiding treatment, as different etiological agents have different intrinsic and acquired drug resistance profiles. Furthermore, accurate taxonomic identification opens possibilities for a deeper understanding of fungal disease epidemiology – uncovering infection spread, their prevalence in various populations, and the factors that contribute to their transmission – enabling us to better identify and protect at-risk groups.[8] Several efforts have pushed medical mycology toward a more modern diagnosis approach such as DNA barcoding. DNA barcoding is the use of a short, universal genetic marker for species identification, and the current barcode sequence for fungal pathogens is the ribosomal internal transcribed spacer (ITS). To date, at least 60 fungal pathogenic species have been targeted by research groups in the development of ITS DNA biosensing strategies for diagnostic purposes.[9–14] To date, over 4000 ITS sequences—belonging to 640 species—are deposited in the ISHAM database of human and animal fungal pathogens.

The large number of species causing fungal disease underlines the mainly opportunistic nature of these infections. Of greater concern is the expansion of certain tropical and subtropical mycosis outside of their endemic regions.[15] Therefore, to address the fungal threat, in addition to being accurate and timely, an ideal diagnostic method should be (1) comprehensive of the fungal interspecies and intraspecies diversity, (2) flexible enough for integration of novel and emerging pathogens in the screening assays (3) portable—requiring minimal instrumentation—and (4) automatable—requiring minimal expertise and avoiding laborious procedures. This can only be achieved through multidisciplinary efforts bringing mycology, molecular biology, and the different branches of engineering.[16] Thus, the goal of this work is to evaluate the prospect of combining fungal DNA barcoding, hybridization-capture biosensing, magnetic labeling, and magnetoresistive DNA detection in the design of fungal diagnosis strategies.

In this work, we used 1239 sequences retrieved from the ISHAM-ITS reference database, belonging to 58 pathogenic fungal species, first to assess the in silico taxonomic coverage of the universal panfungal primers, and then to calculate the expected hybridization sensitivity (% of isolates within a given species displaying ITS DNA complementarity to a specific ITS probe) and specificity (% of strains outside a species of interest without DNA complementarity to the referred species) values for 98 specific fungal probes gathered from the literature. We developed specific hybridization probes for identification of the major yeast pathogens *Candida albicans*, *Candida auris*, *Nakaseomyces gabratus*, and *Cryptococcus neoformans* to be coupled with giant magnetoresistance (GMR) biosensors and implemented in a magnetoresistive detection strategy on a portable and automatable platform. In this work, we further optimized the magnetoresistive detection assay toward the detection of low amounts of fungal DNA, obtaining a limit of detection of 600 sequences per hybridization assay.

2 | MATERIALS AND METHODS

2.1 | Construction of a multiple alignment representing a large virtual pool of clinical isolates

A list of ribosomal internal transcribed spacer (ITS) probes developed for molecular identification of pathogenic fungi and available in the literature (Table 1) was selected for in silico evaluation of hybridization sensitivity and specificity.

A multiple alignment of the ribosomal DNA ITS sequences for 1239 strains belonging to all 58 fungal pathogenic species with published ITS probes[9–14] was computed on the Unipro UGENE software using the MUSCLE algorithm.

All ribosomal ITS sequences deposited in the ISHAM-ITS database (Table S1), corresponding to clinical and veterinary isolates of *Alternaria alternata, Aspergillus fumigatus, Aspergillus sydowii, Aspergillus versicolor, Candida albicans, Candida auris, Candida chodatii, Candida dubliniensis, Candida haemulloni, Candida inconspicua, Candida intermedia, Candida membranifaciens, Candida norvegica, Candida parapsilosis, Candida santamariae, Candida tropicalis, Candida zeylanoides, Clavispora lusitaniae, Cyberlindnera jadinii, Debaryomyces hansenii, Diutina catenulate, Diutina rugosa, Kazachstania exigua, Kazachstania pintolopesii, Meyerozyma guilliermondii, Millerozyma farinose, Nakaseomyces glabratus, Pichia fermentans, Pichia kudriavzei, Pichia membranifaciens, Torulaspora delbrueckii, Wickerhamomyces anomalus, Yarrowia lipolytica, Zygoascus hellenicus, Cladosporium cladosporioides, Epidermophyton floccosum, Histoplasma capsulatum, Kodamaea ohmeri, Lachancea fermentati, Lodderomyces elongisporus, Microsporum audouinii, Microsporum canis, Paracoccidioides brasiliensis, Penicillium chrysogenum, Penicillium marneffei, Priceomyces carsonii, Rhodotorula glutinis, Rhodotorula mucilaginosa, Saccharomycopsis fibuligera, Scheffersomyces spartinae, Sporothrix schenckii, Stachybotrys chartarum, Talaromyces marneffei, Trichophyton mentagrophytes, Trichophyton mentagrophytes, Trichophyton rubrum, Trichophyton schoenleinii, Trichophyton tonsurans, Trichophyton verrucosum, Trichosporon asahii*, and *Trichophyton inkin* were downloaded on February 2024. ITS sequences for *Cryptococcus albidus, Cryptococcus laurentii*, and *C. neoformans* were retrieved from the NCBI genome database.

The 1239 aligned ITS sequences were screened for the presence of complementary regions to the considered probes. Two levels of identity were evaluated: 100% and 90%. Each probe's performance was evaluated based on its ability to target specific fungal taxa and its potential cross-hybridization with non-target species. The same alignment and screening method was used to evaluate the coverage of the pan-fungal primers designed by White et al.[17]

2.2 | Biological and biochemical reagents

Panfungal primers flanking the ITS1 region (FW 5′-biotin TCCGTAGGTGAACCTGCGG 3′ and RV 5′ GCTGCGTTCTTCATCGATGC 3′) and specific probes (*N. glabratus*: 5′-thiol CTACTAAAAGAAATCTTGTGTTGACTGAATTA 3′, *C. auris*: 5′-thiol TAGTTGAACTTAACGTTGGGTTAG 3′, *C. albicans*: 5′-thiol TAATAATCTGGTGTGACAAGTTGATAAA 3′, and *C. Neoformans*: 5′-thiol TACATTCATTACATTTAGAAGTTTGTGTA 3′) were synthesized by Stab Vida.

For DNA labeling, streptavidin-coated magnetic nanoparticles nanomag-D—75%–80% (w/w) magnetite in a dextran 40 kDa matrix, 250 nm diameter, magnetic moment of $\sim 1.6 \times 10^{-16}$ Am^2 for a 1.2 kA/m magnetizing field, and susceptibility of $\chi = 4$—were purchased from Micromod.

Tris EDTA (TE) buffer was prepared with KH_2PO_4 (0.1 mM), Tris (10 mM), EDTA (1 mM), and pH adjusted using HCl (1 M) to 7.4. Phosphate buffer (PB) was prepared from stock solutions of Na_2HPO_4 and NaH_2PO_4 at 0.2 M and pH 7.2. PB-Tween20 was prepared by adding 0.02% (v/v) of Tween 20 from Promega to the PB.

2.3 | Strains and growth media

Laboratorial reference strains of *N. glabratus*, *C. auris*, *C. albicans*, and *C. neoformans* were used in the hybridization and cross-hybridization assays (Table 2).

Clinical isolates provided by Santa Maria Hospital (Lisbon, Portugal) and São João Hospital (Porto, Portugal) were used to further evaluate probe sensitivity. Note that 30 *N. glabratus* clinical isolates (Table S2) were selected out of a larger collection of clinical specimens.[18] Cells were batch-cultured at 30°C with orbital agitation (250 rpm) in YPD growth media, with the following composition (per liter): 20 g glucose (Merck), 20 g yeast extract (Difco), and 10 g peptone (Difco). Solid media contained 20 g/L agar (Iberagar) besides the ingredients listed above.

2.4 | DNA extraction and amplification through asymmetric PCR

DNA was extracted through bead beating and centrifugation. Briefly, cell biomass was suspended in 200 µL of lysis buffer (Tris 50 mM, EDTA 50 mM, NaCl 250 mM, SDS 0.3%), rapidly agitated in a 2-mL tube with 2-mm glass

TABLE 1 Hybridization capture ITS probes retrieved from literature.

A. sydowii	AGACTGCATCACTCTCAGGCATGAAGTTCA	2017 Libert
A. versicolor	AGACTGCATCACTCTCAGGCATGAAGTTCA	2017 Libert
C. albicans	ATTGCTTGCGG CGGTAACGT CC	1998 Elie
	TTATCAACTTGTCACACCAGATTATTACT	2007 Leaw
	TTGCGGCGGTAAGGTCCA	2023 Lin
C. auris	CCACCGCGAAGATTGGTG	Theill 2017
	CGGTGGCGTTGCATTCA	2018 Arastehfar
	TTTGTGAATGCAACGCCATCG	Carolus 2021
	GGTGGCGTTGCATTCACA	2023 Lin
C. chodatii	AGCTCTTAGTTCAGTCCATTCGAAAAGT	2007 Leaw
C. dubliniensis	AAGGCGGTCTCTGGCGTCGCCC	1998 Elie
	AAACTTGTCACGAGATTATT	2007 Leaw
	CTGGCGTCGCACATTTTA	2023 Lin
C. haemulloni	CCGTTGGTGGATTTGTTTCTAA	1998 Elie
	AATCAACCACCGTTAAGTTCAA	2007 Leaw
	CCGTTGGTGGATTTGTTTCT	Theill 2017
C. inconspicua	AGAGAGCGAACTATAAAACGCGC	2007 Leaw
C. intermedia	GTTGTCGCAATACGTTACTTCAACTTTATT	2007 Leaw
C. membranifaciens	AACTGGGGCAGTAAATTTCTAGTAATTGG	2007 Leaw
C. norvegica	ACGAGCGTCTGCTGGCTCCACA	1998 Elie
	TAGCCGGAGACTACAACCAAACTAATTT	2007 Leaw
C. parapsilosis	ACAAACTCCAAAACTTCTTCCA	1998 Elie
	TTCCACTCATTGGTACAAACTCCAAAACTT	2007 Leaw
	TTTGGTAGGCCTTCTATATGGGGCCT	2007 Leaw
	TTAACTGCGACCCTTTTCTTTCTACACA	2007 Leaw
	CCTATCCATTAGTTTATACTCCG	2023 Lin
C. santamariae	GACCAGTAAAGTATTTG	2007 Leaw
C. tropicalis	AACGCTTATTTTGCTAGTGGCC	1998 Elie
	ACTCATTTTAAGCGACTTAG	2007 Leaw
	AACGCTTATTTTGCTAGTGGCC	2023 Lin
C. zeylanoides	GAGCAGTATAGTATTTG	2007 Leaw
C. lusitaniae	CTCCGAAATATCAACCGCGCTG	1998 Elie
	TCAAACACGTTTACAGCACGACATTTC	2007 Leaw
	ACACTTTGCATTTGCGAAC	2023 Lin
C. jadinii	ACTCGTTATTTTCCAGACAGAC	1998 Elie
	CAACTCGTTATTTTCCAGACAGACT	2007 Leaw
D. hansenii	GGCCAGAGGTTTACTGAA	2007 Leaw
D. catenulate	AAAGTGATTGGTGTAGTATTACAGTTTACT	2007 Leaw
D. rugosa	AG TTA AGC TTG TTA CAG ACT CA	1998 Elie
	CGCGACCGTCTAAAACAGTTAAGCTTG	2007 Leaw
K. exigua	GGTTGTTGCAGCTTATAGTTTTTGTGTAAT	2007 Leaw
K. pintolopesii	ACGTCTTCGTAGTAGGTTCTGCCAATT	2007 Leaw
M. guilliermondii	CCCGGCCTTACAACAACCAAAC	1998 Elie
	GTGCTGTCGACCTCTCAATGT	2007 Leaw
	GTCGGACTAGGCGTTTGCT	2023 Lin
M. farinose	TTTACAGTAGATAAATGCCGTTTGACTCTT	2007 Leaw

(Continues)

TABLE 1 (Continued)

N. glabratus	TAGGTTTTACCAACTCGGTGTT	1998 Elie
	TTTACCAACTCGGTGTTGATCT	1998 Elie
	TGGGAGTGTGCGTGGATCTCTCTATTCCAA	2007 Leaw
	TTCGTTTTAGGTGTTGGGCAGTA	2007 Leaw
	GGAGCCGACAAAGACCTGG	2023 Lin
P. fermentans	AAAGCGAGGGGCCTTCTGCGCG	1998 Elie
	GCGAGGGGCCTTCTGCGCGAAC	1998 Elie
P. kudriavzei	AGCGGACGACGTGTAAAGA	2023 Lin
	GGCCCGAGCGAACTAGACTTTT	1998 Elie
	TGTGGAATATAGCATATAGTCGACAAGAGA	2007 Leaw
P. membranifaciens	AAGAAACGTTGCGGACGAAGCG	2007 Leaw
T. delbrueckii	ATTTTTCTGGCTTGGATGACTTTGT	2007 Leaw
W. anomalus	ATCAGCTAGGCAGGTTTAGAAG	1998 Elie
	ATATTGACTTAGCAAGAGT	2007 Leaw
Y. lipolytica	CTCAATGATTACGTCATTTCACC	2007 Leaw
Z. hellenicus	TTAAGCACAATTTTCTGAAATACATTGGTG	2007 Leaw
C. cladosporioides	CCGGGATGTTCATAACCCTTTGTTGTCC	2017 Libert
C. albidus	CTAAAGACCGCTTTCTAATCCATTGATCT	2007 Leaw
C. laurentii	ACCTCTGTGAACTGTGGACC	2007 Leaw
C. neoformans	CCTATGGGGTAGTCTTCGG	2001 Lindsley
	TTTTATTACCTGTTGGACTTGGATT	2007 Leaw
	GTTGGACTTGGATTTGGGTGTT	2023 Lin
E. floccosum	CCATAGGTGGTTCAGTCTGAGCGT	2007 Li
H. capsulatum	ACCATCTCAACCTCCTTTTTCACACCAGG	2001 Lindsley
K. ohmeri	GACGACAGTACTCTACAAAACGGTACC	2007 Leaw
L. fermentati	TGAGTGGACGCTACAAAG	2007 Leaw
L. elongisporus	AACCACTCCATTGTGCTTAATAAAAAGC	2007 Leaw
M. audouinii	CGACCGTCCCCCCCCAATAAC	2007 Li
M. canis	CCAACTCCCCAGTAACCACCCACC	2007 Li
P. brasiliensis	CACTCATGGACCCCGG	2001 Lindsley
P. chrysogenum	GCCTGTCCGAGCGTCATTTCTGCCCTCAAGC	2017 Libert
P. marneffei	GACGCGCAGCTCTTTTTA	2001 Lindsley
P. carsonii	TTGCTTTGGCTTGTCTCTAGA	2007 Leaw
R. glutinis	TAGTGAATCTGGTGGTGCTTG	2007 Leaw
R. mucilaginosa	TAATGATTGAAGAGGTGTTTGG	2007 Leaw
S. fibuligera	GATTGAGTTTTCCATATATTTGCTTAAGGA	2007 Leaw
S. spartinae	AATACAGCGCACTCGACAATCA	2007 Leaw
S. schenckii	GGGTTGGTCACCACCATA	2001 Lindsley
S. chartarum	CTGCGCCCGGATCCAGGCGCCCGCCGGAGA	2017 Libert
T. marneffei	ATGGGGCTCTGTCACTCGCTC	2023 Lin
T. mentagrophytes	GCCCCCGTCTTTGGGGGTGCG	2007 Li
T. mentagrophytes	ATAGGGACCAACGTTCCGTCAGGG	2007 Li
T. rubrum	GCAGCCAATYCAGCGCCCT	2007 Li
	CAGACACCAAGAAAAAATTCTCTG	2007 Li
T. schoenleinii	CGAATGGGCGCAACAAACCA	2007 Li
T. tonsurans	TCCGGCTTTCTAGGCGA	2007 Li
T. verrucosum	TAGGGATCAGCGTTCCATCA	2007 Li
T. asahii	ATATCCACTTACACCTGT	2007 Leaw
T. inkin	TTGACATTCATGTCTGG	2007 Leaw

TABLE 2 Genotypes and ITS1 sequences of *C. albicans*, *C. auris*, *N. glabratus*, and *C. neoformans* type strains used in on-chip hybridization and cross-hybridization assays.

Strain	Genome assembly	ITS1 sequence
C. albicans ATCC 18804	GCF_000182965.3	TCCGTAGGTGAACCTGCGGAAGGATCATTACTGATTTGCTTAA-TTGCACCACATGTGTTTTTCTTTGAAACAAACTTGC-TTTGGCGGTGGGCCCAGCCTGCCGCCAGAGGTCT-AAACTTACAACCAATTTTTTATCAACTTGTCACACCAGATT-ATTACTTAATAGTCAAAACTTTCAACAACGGATCTCTTGGTTC-TCGCATCGATGAAGAACGCAGC
C. auris B11221	GCA_003013715.2	TCCGTAGGTGAACCTGCGGAAGGATCATTATTGATATTTTGCA-TACACACTGATTTGGATTTTAAAACTAACCCAACGTTAAGTT-CAACTAAACTATAAAGAAAACTTTCAACAACGGATCTCTTGGTT-CTCGCATCGATGAAGAACGCAGC
N. glabratus ATCC 2001	GCA_010111755.1	TCCGTAGGTGAACCTGCGGAAGGATCATTAAAGAAATTTAA-TTGATTTGTCTGAGCTCGGAGAGAGACATCTCTGGGGAGGACC-AGTGTAGACACTCAGGAGGCTCCTAAAATATTTTCTCTGCTGTG-AATGCTATTTCTCCTGCCTGCGCTTAAGTGCGCGGTTGGTGGG-TGTTCTGCAGTGGGGGGAGGGAGCCGACAAAGACCTGGGAG-TGTGCGTGGATCTCTCTATTCCAAAGGAGGTGTTTTATCACAC-GACTCGACACTTTCTAATTACTACACACAGTGGAGTTT-ACTTTACTACTATTCTTTTGTTCGTTGGGGGAACGCTCTCTTTC-GGGGGGGAGTTCTCCCAGTGGATGCAAACACAAACAAATATT-TTTTTAAACTAATTCAGTCAACACAAGATTTCTTTTAGT-AGAAAACAACTTCAAAACTTTCAACAATGGATCTCTTGGTTC-TCGCATCGATGAAGAACGCAGC
C. neoformans H99	GCA_011801205.1	TCCGTAGGTGAACCTGCGGAAGGATCAGTAGAGAATATTGGAC-TTCGGTCCATTTATCTACCCATCTACACCTGTGAACTGTTTA-TGTGCTTCGGCACGTTTTACACAAACTTCTAAATG-TAATGAATGTAATCTTATTATAACAATAATAAAACTTTCAAC-AACGGATCTCTTGGCTTCCACATCGATGAAGAACGCAGC

beads for 30 s, and incubated for 1 h at 65°C. The lysate was centrifuged for 15 min at 13,000 rpm, 4°C to remove cell debris, and the supernatant DNA was precipitated with 1/10 NaCl and 2 volumes of ethanol, for 30 min at −20°C. The DNA pellet was washed with ethanol two times and resuspended in nuclease-free water.

The genomic rDNA ITS region was amplified trough asymmetric PCR using a 10:1 (FW/RV) primer ration. PCR reactions were performed in a 50 µL final volume containing 50 ng template DNA, 5 µL reaction buffer, 2.5 µL $MgCl_2$, 0.8 µL dNTPs (10 mM), 1 µL NZYTaq II DNA polymerase (NZYtech), 1 µL of forward primer (10 µM), 1 µL of reverse primer (1 µM), and nuclease-free water. A negative control (no template control) was included in all amplifications. The ITS-rDNA amplification was carried out with an initial denaturation at 95°C for 2 min, followed by 55 cycles of 94°C for 30 s, 57°C for 30 s, and 72°C for 16 s, concluding with a final extension at 72°C for 10 min. The final concentration of single-stranded DNA was accessed with a spectrophotometric method on NanoDrop One. Five microliters of amplified target DNA from each reaction tube was electrophoresed at 150 V in TAE buffer and a 1% agarose gel stained with GreenSafe (NZYtech). Bands were visualized using a gel imaging and documentation system.

2.5 | Biochips

Each biochip features an array of 30 spin-valve sensors coated with an oxide passivation layer, organized into six sensing regions, each containing five active sensors. The sensor microfabrication is described in the work of Martins et al.[19]

For this work, the SV stack, Ta 2.0 nm/NiFe 2.5 nm/CoFe 2.8 nm/Cu 2.6 nm/CoFe 2.4 nm/MnIr 7.0 nm/Ta 5.0 nm, was deposited in a 150 mm Si/SiO_2 100 nm wafer. The sensors are configured as two spin valves (active area: 80×2.6 μm^2) electrically connected by aluminum leads. The magnetic response was characterized, with an average MR of 6.0% and a sensitivity of 1.3%/mT.

2.6 | Magnetoresistive platform

Envisioning a point-of-care approach, the sensors described above were used in conjunction with a portable platform developed by Martins et al. combining an electronic set-up and a microfluidic system for sample loading. The detection platform has already been validated for detecting cell-free nucleic acids,[20] proteins,[21] bacteria,[22]

and nematodes.[23] The platform comprises three different parts: (1) a power supply/battery, (2) a control and acquisition board bridging the device and the user interface, and (3) a magnetic field generator/inductor. For real-time monitoring, the biochip is inserted into the platform via a designated slot, and the platform is connected to a computer via USB. For the measurement setup and real-time monitoring of the assays, a user interface software is available. More detail on the platform electronics can be found in Martins et al.[24]

2.7 | On-chip hybridization, magnetic labeling, and DNA detection

The probes designed for *N. glabratus*, *C. auris*, *C. albicans*, and *C. neoformans* detection were diluted in TE buffer to an empirically optimized concentration of 5 nM for *C. neoformans* and 1 nM for the other species. The biochip's surface was cleaned and 0.5 µL of specific ITS probe probe was manually spotted over the sensing area. Note that 0.5 µL BSA 1% (w/v) was spotted for background correction. The immobilization of thiolated probes on the gold sensors was carried in a humid chamber at 37°C for 1 h. The functionalized biochip was coupled with a PDMS microfluidic channel, and inserted into the magnetoresistive platform, connected to a computer running the data acquisition software. Sensors were washed with PB to remove unbound probes, loaded with 10 µL of amplified target ITS DNA for 30 min of stationary hybridization, and washed again to remove unbound targets. After a 2-min baseline voltage reading, labeling paramagnetic particles were injected in the system and left for 10 min stationary binding. A final round of washing removed unbound nanoparticles, resulting in a final voltage less than or equal to the baseline.

Reagents were loaded with a syringe pump, at a flow rate of 50 µL/min, and washed at a flow rate of 10 µL/min. The sensors were biased applying a 1 mA DC current. An external AC magnetic field of 13.5 Oe at 211 Hz was applied to magnetize the superparamagnetic labeling nanoparticles.

2.8 | Evaluation of test sensitivity, specificity, and limit of detection

As explained in Martins et al.,[19] and according to the type of assay used (Figure 1), the presence of the target analyte will create a decrease in the measured resistance and consequently in the measured voltage. Thus, for each sensor, the final voltage measurement (post-sample introduction) is subtracted from the baseline voltage measurement (pre-sample introduction) and the difference is normalized to the baseline. Sensors with low baseline ($v < Q1 - (0.5 \times IQR)$) and low saturation signal ($\Delta v\% < Q1 - (1.5 \times IQR)$) were removed. Each value was corrected against a negative control.

Complementary DNA hybridization assays included the results obtained from testing (1) *N. glabratus* ITS capture probe against amplified *N. glabratus* ITS DNA, (2) *C. auris* ITS capture probe against amplified *C. auris* ITS DNA, (3) *C. albicans* ITS capture probe against amplified *C. albicans* ITS DNA, and (4) *C. neoformans* ITS capture probe against amplified *C. neoformans* ITS DNA. Non-complementary or cross-hybridization assays were performed to assess the specificity of each probe. The number of positive results in complementary DNA assays (true positive), negative results in non-complementary DNA assays (true negative), positive results in non-complementary DNA assays (false positive), and negative results in complementary DNA assays (false negative) were used to infer test's sensitivity (true positives/(true positives+false positives) × 100) and specificity (true negatives/(true negatives+false positives) × 100). The equality of group variances was analyzed with Welch ANOVA and ad hoc Tukey's multiple comparisons test. To determine the limit of detection, 1 µM, 1 nM, 1 pM, and 1 fM of target *N. glabratus* ITS DNA were hybridized to 1 nM of immobilized ITS probe, magnetically labeled and detected as described in the previous section. The lowest amount of detected DNA (1 fM) was evaluated against 1 nM of ITS capture probe on six chips, corresponding to 60 sensors, and compared to a blank control (absence of DNA target) on-chip. The limit of detection analysis was performed for *N. glabratus* ITS-DNA only.

3 | RESULTS

3.1 | Evaluation of fungal universal primers and specific probes suitable for 58 fungal species, covering a variety of over 1000 strains

A total of 98 specific fungal ITS probes were retrieved from nine research articles published from 1998 to 2023. The set of probes covered 35 genera and 58 species (Figure 2) with in silico hybridization sensitivity ranging from 0% to 100%, and specificity ranging from 95% to 100%. Among the published probes, 61% targeted *Candida* or yeast species formerly included in the *Candida* genus, and 12% targeted rare, cryptic, or usually non-pathogenic yeast. The average probe sensitivity was 70% for *Candida*, 78% for respiratory infection yeasts and moulds, 65% for dermatophytic fungi, and 65% for cryptic pathogens.

ITS probes allowing for 100% hybridization sensitivity and specificity were identified for the major fungal pathogens *A. fumigatus*, *C. auris*, *C. dublinensis*,

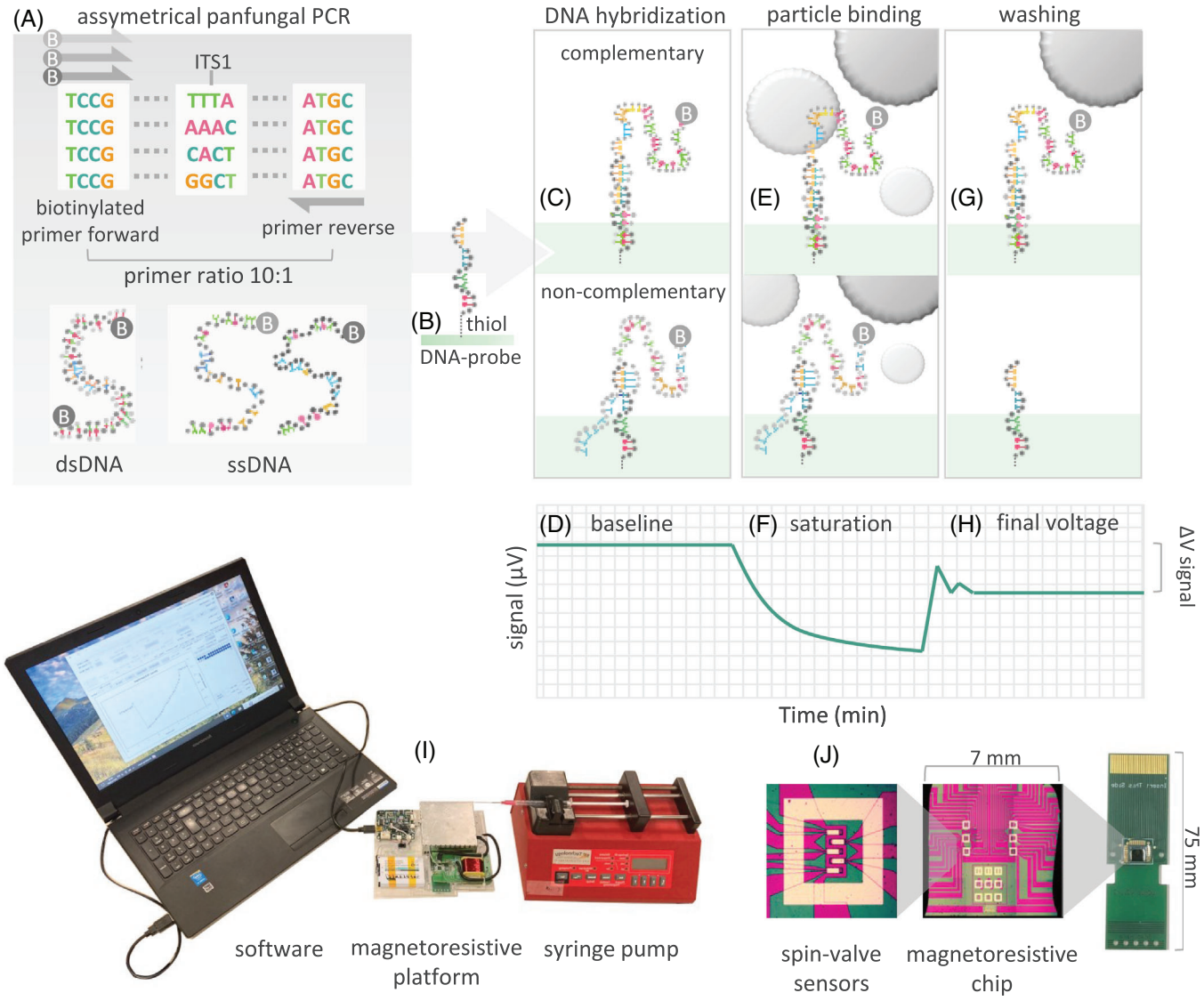

FIGURE 1 Magnetoresistive biosensing assay. First, the biotinylated ssDNA generated through asymmetrical PCR (A) is hybridized to a complementary DNA capture-probe (B) immobilized on the chips surface (C). A bias current is applied to generate a baseline signal (D). Streptavidin-coated paramagnetic nano-particles are loaded (E) to generate a saturation signal (F). A final washing step (G) removes non-complementary DNA and unbound nanoparticles. The retained paramagnetic particles generate a magnetoresistive signal (h), measured by the difference between the final and the initial voltage signals. To perform the assays, the chip is inserted in the magnetoresistive platform, coupled to a personal computer equipped with the data acquisition software and to a syringe pump for sample loading (I). The magnetoresistive sensing regions are grouped in patches of five spin valves. The biochip sensors (J) are arranged in six sensing regions, each one containing five active sensors covered with a gold layer, and surrounded by a gold frame.

C. parapsilosi, *E. floccosum*, and *T. rubrum*. Great disagreement between strains deposited in the worldwide database and identification probe was observed for the endemic pathogens *H. capsulatum* and *P. brasiliensis*, and the rare pathogens *C. zeylanoides* and *Y. lipolytica*. For the commonly isolated pathogenic yeast *C. albicans*, *N. glabratus*, and *D. hansenii*, for which around 100 genomes are available, and for *C. tropicalis*, *D. rugosa*, and *Cryptococcus* species, probes enabling accurate detection of 100% of the strains were not identified in the literature.

The advantage of using ribosomal sequences for diagnostics is its simplicity and inclusiveness as one single primer set could theroeticaly amplify the ribosomal genes of virtually any microbial species. In 1990, White used the highly conserved ribosomal regions to design sets of universal primers for PCR amplification of rDNA genes in fungi.[15] The adequacy of the primers flanking the highly variable ITS1 region was tested against all ISHAM database sequences, for the 58 fungal species mentioned above. Among these sequences, 34 harbor mismatches at the

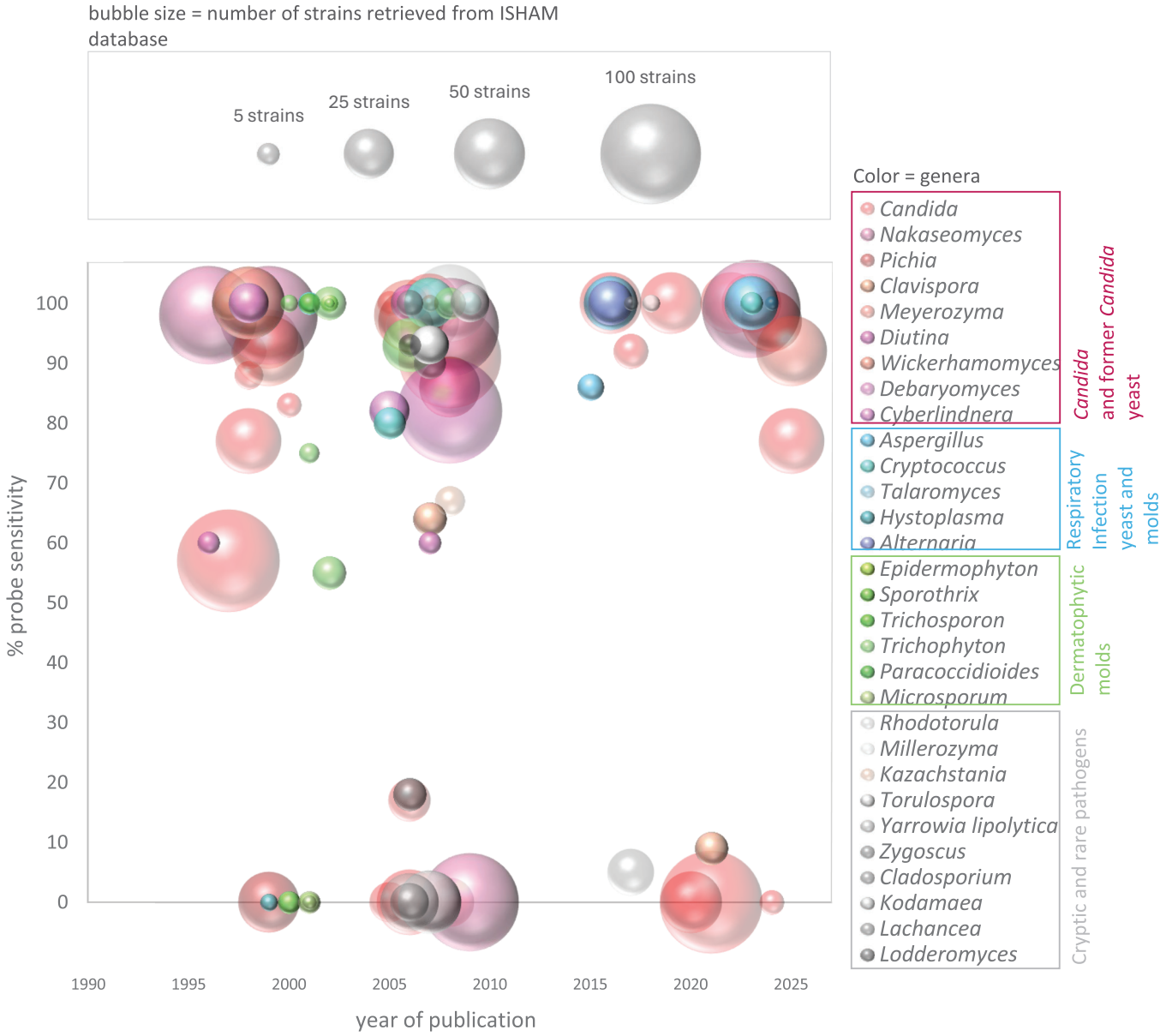

FIGURE 2 Literature probes review. Bubble plot illustrates the sensitivity (*y*-axis) of fungal barcode hybridization probes proposed from 1998 to 2023 (*x*-axis) against the number of clinical strains whose ITS sequence is available at ISHAM database (bubble size) and grouped in pathogenic profile (color).

forward primer regions, including four highly mutated *C. albicans* strains, namely, CBS2688, CBS5983, CBS4908, and CBS2696, which display seven mismatches each. At the reverse primer region, all *P. kudriavzevii*, *P. fermentans*, and *C. inconspicua* strains share a point mutation (A–G transition) at the 14th position, all *C. norvegica* strains have a T–A transversion at the fourth position, *D. rugosa* has a C–T transition at the seventh position, and all *Yarrowia lipolytica*, *Histoplasma capsulatium*, *P. brasiliensis*, and *C. neoformans* have a G–A transition at the first position. Overall, the panfungal primers seem to be capable of amplifying the ITS1 region of 98.5% of the ISHAM database strains, including common and cryptic pathogens, assuming 90% complementarity as threshold for primer annealing.

3.2 | Design and test of specific probes for on-chip hybridization capture of four pathogenic yeast species achieving >95% accuracy

Specific hybridization probes for identification of *N. glabratus*, *C. auris*, *C. albicans*, and *C. neoformans* were designed using the UGENE software by screening for a 30-basepair long region common to >95% of all strains within

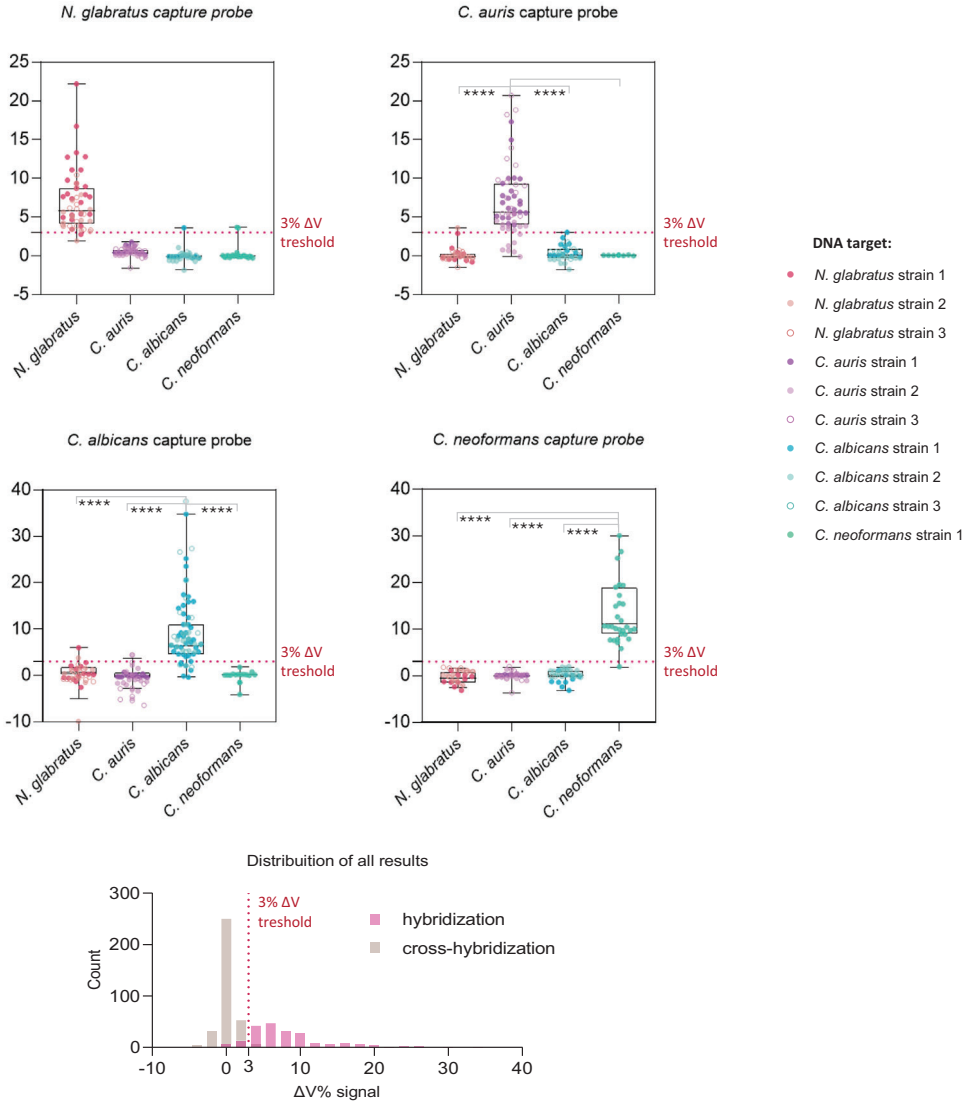

FIGURE 3 On-chip target-probe hybridization and cross-hybridization assays. Assays were performed for three strains of *N. glabratus*, *C. auris*, *C. albicans*, and *C. neoformans*. Each hybridization chip harbors 30 magnetoresistive sensors, and each colored circle represents the Δv% signal value measured by one sensor. Note that 96% of sensors generating a Δv% signal >3 corresponded to truly positive detection events, and 95% of sensors generating a Δv% < 3 corresponded to truly negatives, leading to an estimated hybridization accuracy of 95%. ****p-value < 0.0001 (Tukey's multiple comparisons test).

each species, imposing a 100% match search algorithm, and exclusive to >95% of all strains within each species, imposing 70% match search algorithm. The 30-basepair long region nearest to the forward primer was selected, and the length of the probes was adjusted to equalize the melting temperature of the set (52.5°C ± 0.5).

Evaluation of the novel data set against the ITS DNA sequences from 1239 isolates, belonging to 58 species, revealed an average in silico sensitivity of 99% when searching for 100% complementarity and 100% when searching for 90% complementarity, and an average in silico specificity of 100%.

During on-chip assays, DNA hybridization was detected with magnetoresistive sensors, through the fringe field generated after paramagnetic DNA labeling. A positive detection event produced, on average, a signal of 6.9 Δv% for *N. glabratus* probe-target hybridization (with 95% of hybridization events producing a Δv% > 3), 7.0 Δv% for *C. auris* probe-target hybridization (95% > 1 Δv%), 8.5 Δv% for *C. albicans* probe-target hybridization (95% > 2 Δv%), and 12.6 Δv% for *C. neoformans* probe-target hybridization (95% > 7 Δv%). Unspecific probe-target combinations resulted in an average signal of 0.16 Δv% (90% < 1.5 Δv%) (Figure 3). The difference between positive hybridization signal and unspecific DNA binding was found significant, supported by a p value < .0001 (Welch t-test).

To determine the classifier threshold for a positive result, we analytically identified the signal value that minimizes

TABLE 3 Comparison between the FDA-cleared methods and the emerging magnetoresistive technology.

	Affirm VPIII	YTL PNA FISH	T2Candida	On-chip
Target	*Candida* species, *Gardnerella vaginalis*, *Trichomonas vaginalis*	*Candida*, *Nakaseomyces*, and *Pichia*	*C. albicans*, *C. tropicalis*, *C. parapsilosis*, *P. kudriavzevii*, and *N glabratus*	*C. albicans*, *C. auris*, *N. glabratus*, and *C. neoformans*
Sample type	Vaginal fluid specimens	Positive blood	Whole blood	Cell culture
NA labeling	Enzymatic	Fluorescent	Magnetic	Magnetic
Resolution	Genus (*Candida*)	Genus	Species level	Species level
Specificity	99%	98%	91%	98%
Sensitivity	83%	97%	94%	91%
Limit of detection	10^4 cells/mL	10^5 cells/mL	1 cell/mL	600 ssDNA strands
Pre-processing	Integrated	NA	Integrated	Benchtop
Requirements	BD Affirm VPIII Processor	Fluorescence microscope	T2Dx Instrument	Magnetoresistive platform
Device cost €	28,000	NA	140,000	2000
Device wight	3.6 kg	NA	145 kg	<1 kg
Cost per assay €	~60	~80	~200	20

erroneous outcomes (false positives and false negatives) based on individual sensor outputs. Above a 3.0 Δv% signal threshold, the estimated accuracy was of 95%, estimated on-chip sensitivity (true positive rate) was 91%, and on-chip specificity (true negative rate) was 98%.

Our results are comparable to the FDA-cleared nucleic acid yeast diagnostic methods such as the PNA-FISH yeast traffic light (with 97% sensitivity and 98% specificity),[25] the affirm VPIII (with 83% sensitivity and 99% specificity),[26] and the T2Candida (with 91% sensitivity and 94% specificity).[27]

Affirm VPIII, PNA-FISH yeast traffic light, and Candida T2 diagnostic tests are performed directly on the clinical sample. Affirm VPIII identifies only *C. albicans*, differentiating candidiasis from bacteriosis, although with some cross-reactivity with *Cryptococcus*. PNA-FISH yeast traffic light targets rRNA, differentiating yeast at a genus level (*Candida*, *Nakaseomyces*, and *Pichia*). The Candida T2 diagnostic test can identify and differentiate at a species level *C. albicans*, *C. tropicalis*, *C. parapsilosis*, *P. kudriavzevii*, and *N. glabratus*, on the T2Dx Instrument, integrating a built-in thermocycling module for pan-Candida amplification and weighting 145 kg. A summarized comparison between the FDA-cleared methods and the emerging magnetoresistive technology is provided in Table 3.

Emphasizing miniaturization and portability, our on-chip DNA-hybridization assays were performed on a microfluidic channel, within a volume of 1 µL. Magnetoresistive detection of specific DNA sequences was achieved at room temperature and on a portable instrument. The feasibility of integrating upstream DNA extraction and amplification modules while retaining compactness is within the future perspectives.[16] For the time of this work, what separates the magnetoresistive fungal barcoding diagnostic assay from the clinical reality and from point-of-care applications is the reliance on an external thermocycling device. However, various approaches for miniaturized DNA amplification have already been demonstrated,[14,28] and we expect to integrate such a solution into our system in the near future.

3.3 | Assessing sensitivity based on the testing of 30 unsequenced *N. glabratus* clinical isolates

To further interrogate the clinical value of the devised biosensing diagnostic strategy, DNA extracted from 30 clinical isolates was subjected to panfungal ITS amplification and on-chip identification. Each strain was tested for hybridization on one magnetoresistive chip harboring 10(±3) sensors. For each strain, the average Δv% of 10(±3) measurements was considered. The average Δv% signal for all strains was 7.2%. All 30 isolates were successfully detected, with each strain achieving an average Δv% detection signal superior to the threshold defined in the previous section (Section 3.2) for the most accurate species differentiation (>3Δv%) (Figure 4).

Complementing the in silico probe accuracy analysis performed against 1239 strains (Section 3.1), the on-chip hybridization results further validate the sensitivity of the devised probing strategy for identifying *N. glabratus*, a drug-resistant[5] pathogen with remarkably high mutagenic rates.[29] These results prove the robustness and

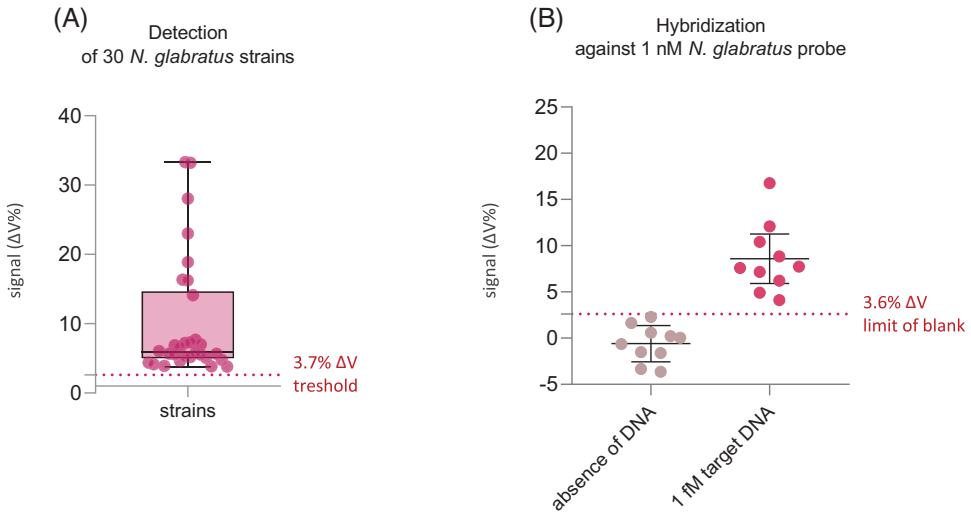

FIGURE 4 Sensitivity and limit of detection. (A) Sensitivity of the on-chip hybridization detection assay, demonstrated by positive signal (Δv%, x-axis) obtained upon hybridization assays with all the 20 clinical strains tested (red circles) against *N. glabratus* specific ITS probe. (B) Femtomolar detection limit was demonstrated by positive signal (Δv%, y axis) obtained on 10 hybridization assays with target ITS DNA diluted to 1 fM (600 sequences/μL), compared to a blank control. Each circle mark corresponds to the average normalized Δv% signal (10 giant magnetoresistance [GMR] sensors) for each performed hybridization assay.

comprehensiveness of the assay for intraspecific pathogen diversity.

3.4 | Assessing the limit of detection of the constructed biochips

For magnetoresistive DNA detection, femtomolar limits of detection (LOD) were proposed in previous works with synthetic DNA.[19] In experiments with bacterial DNA detection, higher limits were demonstrated,[22] and with viral DNA sequences,[30] an LOD of ~600,000 molecules per 1 μL assay (picomolar) was achieved. In this work, *N. glabratus* ITS DNA was serially diluted to a concentration of 1 fM and hybridized on-chip against 1 nM of specific ITS probe. The average Δv% hybridization signal was 7.9 when target DNA was present, and 0.9 when DNA was absent.

The limit of blank (LOB = μblank + 1.645·σblank) was 2.6%, and thus femtomolar level of detection was achieved in accordance with the WHO guidelines, with a confidence level >95%.

The proposed on-chip DNA-hybridization assays were performed on a microfluidic channel, within a volume of 1 μL, coupled to a compact magnetoresistive detection system[24] connected to a portable computer. It requires previously extracted and amplified DNA. Theoretically, assuming 100% efficiency, 1 single strand of ITS DNA (ITS ssDNA), subjected to five exponential PCR cycles and five linear (asymmetrical) PCR cycles, would generate 1100 ITS ssDNA strands for on-chip hybridization. These results promise the generation of a detection signal after 1 h of assay (15 min PCR, 30 min hybridization, 5 min labeling, and 10 min washing), greatly improving the 2–21 days turnaround time associated with the current gold standard culture-based methods.

Although our experimental work does not address the upstream sample processing procedures such as pathogen capture, lysis, and amplification, our DNA detection results are compared to FDA-cleared probe-hybridization-based yeast diagnostic tests, which offer limits of detection of 10^5 cells/mL (PNA-FISH yeast traffic light), 10^4 cells/mL (Affirm VPIII), and 1 cell/mL (Candida T2 panel), if associated with a prior step of cell capture. Indeed, the greatest challenge for broad implementation of sequence-based infectious disease diagnostic methods in clinical reality is the small number of pathogen cells in human samples.[16] For instance, one pathogenic cell must be detected in several microliters of bodily fluid and efficiently guided into a 25-μL PCR tube, so its DNA can be extracted and amplified. Therefore, to improve limits of detection, molecular methods need to integrate solutions such as immunomagnetic labeling and separation[31] or microfluidic pathogen-trapping architectures[32–34] for sample pre-processing.

4 | DISCUSSION

The most acknowledged genomic sequences for molecular identification of fungi—and any other organism—are the

ribosomal RNA (rRNA) genes. Using ribosomal sequences allows for diagnostics simplicity and inclusiveness, being an amplification of the ribosomal genes of virtually any microbial species theoretically possible with one primer set. For downstream panfungal PCR product identification, the gold standard in DNA barcoding is sequencing. ITS sequencing has played a pivotal role in the discovery of previously undescribed fungal pathogens and in better understanding fungal epidemiology. There are several documented cases where amplification and sequencing of the ITS region have been instrumental in diagnosing fungal infections when other methods failed.[35–37] Sequencing, however, is often expensive and time-consuming. Hybridization capture, on the other hand, is cost-effective, easy to implement in portable biosensor solutions, and has the potential to be equally accurate.

For analyte detection, biosensors usually rely on fluorescent labeling, which traditionally requires sophisticated equipment but can also be miniaturized and combined with microfluidics,[38] enzymatic labeling, which allows for naked-eye readouts,[14,39] label-free systems that significantly simplify the biosensing workflow,[40] and metallic labeling, known for its specificity, particularly useful in single nucleotide polymorphism detection. In this work, GMR-based sensors were chosen for hybridization signal detection due to their (1) high sensitivity for small changes in magnetic fields; (2) small detection fields, enabling multiplexed assays in a small area, (3) absence of intrinsic ferromagnetism in biological samples, which results in reduced background noise, (4) robustness against interferences from environmental factors such as solvent concentration and pH, and (5) integration and miniaturization potential for large-scale integration technologies at reduced cost (in this case, €20 for assay).

In this work, the combination of four highly promising technologies: DNA barcoding, hybridization-capture, magnetic labeling, and GMR detection, resulted in a highly sensitive and specific biosensing assay with promising potential for point-of-care diagnostics. The assay consists of two pipetting steps – one for sample loading and one for sample labeling – on a portable electronic platform, with 30-min waiting time for sample hybridization, 10-min waiting time for sample labeling, and 10 min for washing.

To demonstrate the efficiency and accuracy of the hybridization-barcoding diagnostic strategy, four yeast pathogens classified in the World Health Organization's fungal priority group as top-ranking were addressed. The herein-demonstrated diagnostic system was able to detect and differentiate *C. albicans*, *C. auris*, *N. glabratus*, and *C. neoformans* with 95% accuracy. These results are of high clinical value, as each of these pathogens has its own infection strategy and therapeutic demands. For instance, *C. albicans*, the most common cause of fungal infection, may be treated with fluconazole, while isolates of *C. auris*, *N. glabratus*, and *C. neoformans* display acquired resistance to azole drugs. The front-line treatment for the emerging multidrug-resistant species *C. auris* and *N. glabratus* is micafungin and caspofungin, respectively, and the front-line treatment for the high-mortality pathogen *C. neoformans* is amphotericin B. Furthermore, the biosensing assay was designed to maximize flexibility and ease of multiplexed target species inclusion. Conducting the proposed bioinformatic analysis to avoid cross-hybridization and reference strain bias, followed by probe design and hybridization assay, would make it possible to identify and accurately differentiate as many as all the 640 fungal species deposited in the international medical mycology ISHAM database.

To further interrogate the clinical value of the devised biosensing diagnostic assay, 30 unsequenced clinical specimens of *N. glabratus* had their DNA identified on-chip. This type of assay was prioritized on *N. glabratus* because of this species' high intraspecific diversity and mutagenic rate.[29,41] These results, combined with the low limit of detection and the small reaction volumes, pave the way for the broader application of biosensing technologies in infectious disease control and toward a more ethical and pragmatic infectious disease diagnosis culture.

The current challenges in timely and accurate diagnosis of fungal infections are mostly imposed by the vast diversity of potentially pathogenic fungal species and strains, and the small number of cells in human samples. Following this work, future perspectives of critical importance for revolutionizing fungal diagnosis include the increase in on-chip detection multiplexity for taxonomic coverage of all fungal pathogens, and the implementation of on-chip DNA amplification strategies for a truly portable and decentralized, point-of-care diagnostic solution. The sensitivity and limit of detection of the molecular diagnostic assay are mostly determined by the upstream sample preprocessing workflow—which can occur at the bench-top or be integrated within the DNA detection system—and includes cell capture, DNA extraction, and purification preceding the amplification. Nevertheless, integration of electrically assisted mass transfer to guide the analyte toward the sensing region or even magnetically assisted hybridization could further decrease the limit of detection and time to result.

The presented results represent a milestone in the envisioned modernization of medical mycology by thoroughly evaluating currently existing technologies and proving the feasibility of accurate, timely, scalable, and far-reaching fungal infection molecular–diagnostic assays.

AUTHOR CONTRIBUTIONS

Maria Zolotareva conducted most of the experiments and drafted the manuscript. Francisco Cascalheira, Ruben Afonso, Ana Martins and Maria Corado contributed with specific experiments and data analysis. Cristina Bárbara, Cátia Caneiras, Diogo Caetano and Miguel Teixeira coordinated the work, experiment design and data interpretation. All authors participated in drafting and revising the manuscript and share responsibility for its accuracy and integrity.

ACKNOWLEDGMENTS

This work was supported by the National Funds supported by Fundação para a Ciência e a Tecnologia (FCT) in the scope of the project UIDB/04565/2020 and UIDP/04565/2020 of the Research Unit Institute for Bioengineering and Biosciences (iBB), and the project LA/P/0140/2020 of the Associate Laboratory Institute for Health and Bioeconomy—i4HB, as well as through the financing of pluriannual BASE INESC MN (UID/05367/2020) and PROGRAMATICO (UIDP/05367/2020). Funding was also received from projects EIT Health Innovation Call Bactometer–RIS_innovation-068, MORE4MEDICAL ECSEL/0007/2019, HfPT–Health from Portugal 02/C05-i01.01/2022.PC644937233-00000047, UNLOOC HORIZON-KDT-JU-2023-1-IA-Topic-1 and OSCARS Project FAIRY - FAIRification of YEASTRACT+ to Support Yeast-based Bioeconomy and Health.

CONFLICT OF INTEREST STATEMENT

The authors declare no conflict of interest.

ORCID

Maria Zolotareva https://orcid.org/0009-0006-2607-5459

REFERENCES

1. D. W. Denning, *Lancet Infect. Dis.* **2024**, *24*, e428.
2. S. Uysal, B. Arda, M. I. Taşbakan, Ş. Çetinkalp, I. Y. Şimşir, A. M. Öztürk, A. Uysal, İ. Ertam, *Int. Wound J.* **2017**, *14*, 1219.
3. L. Brown, A. K. Leck, M. Gichangi, M. J. Burton, D. W. Denning, *Lancet Infect. Dis.* **2021**, *21*, e49.
4. M. F. Price, M. T. LaRocco, L. O. Gentry, *Antimicrob. Agents Chemother.* **1994**, *38*, 1422.
5. M. A. Pfaller, D. J. Diekema, J. D. Turnidge, M. Castanheira, R. N. Jones, *Open Forum Infect. Dis.* **2019**, *6*, S79.
6. K. C. Dantas, T. Mauad, C. D. S. De André, A. L. Bierrenbach, P. H. N. Saldiva, *Sci. Rep.* **2021**, *11*, 3943.
7. M. C. Dignani, *F1000Prime Rep.* **2014**, *6*, 81.
8. C.-C. Tsang, J. L. L. Teng, S. K. P. Lau, P. C. Y. Woo, *JoF* **2021**, *7*, 636.
9. C. M. Elie, T. J. Lott, E. Reiss, C. J. Morrison, *J. Clin. Microbiol.* **1998**, *36*, 3260.
10. M. D. Lindsley, S. F. Hurst, N. J. Iqbal, C. J. Morrison, *J. Clin. Microbiol.* **2001**, *39*, 3505.
11. S. N. Leaw, H. C. Chang, R. Barton, J.-P. Bouchara, T. C. Chang, *J. Clin. Microbiol.* **2007**, *45*, 2220.
12. X. Libert, A. Packeu, F. Bureau, N. H. Roosens, S. C. J. De Keersmaecker, *PLoS ONE* **2017**, *12*, e0173390.
13. K. Bieber, M. Harder, S. Ständer, K. Boch, K. Kridin, B. Köhler, W. Anemüller, A. L. Ernst, D. Zillikens, M. Cavalar, R. J. Ludwig, *J. Deutsche. Derma. Gesell.* **2022**, *20*, 1112.
14. C. Lin, H. Tang, X. Hu, G. Li, T. Jiang, W. Yang, Z. Xia, Y. Zhu, H. Xu, J. Zhou, J. Shen, *IDR* **2023**, *16*, 5347.
15. N. Ashraf, R. C. Kubat, V. Poplin, A. A. Adenis, D. W. Denning, L. Wright, O. McCotter, I. S. Schwartz, B. R. Jackson, T. Chiller, N. C. Bahr, *Mycopathologia* **2020**, *185*, 843.
16. M. Zolotareva, F. Cascalheira, C. Caneiras, C. Bárbara, D. M. Caetano, M. C. Teixeira, *Trends Biotechnol.* **2024**, *42*, 1628.
17. T. J. White, T. Bruns, S. Lee, J. Taylor, in *PCR Protocols*, Elsevier, **1990**.
18. C. Costa, C. Pires, T. R. Cabrito, A. Renaudin, M. Ohno, H. Chibana, I. Sá-Correia, M. C. Teixeira, *Antimicrob. Agents Chemother.* **2013**, *57*, 3159.
19. V. C. Martins, F. A. Cardoso, J. Germano, S. Cardoso, L. Sousa, M. Piedade, P. P. Freitas, L. P. Fonseca, *Biosens. Bioelectron.* **2009**, *24*, 2690.
20. T. M. Dias, F. A. Cardoso, S. A. M. Martins, V. C. Martins, S. Cardoso, J. F. Gaspar, G. Monteiro, P. P. Freitas, *Anal. Methods* **2016**, *8*, 119.
21. D. C. Albuquerque, V. C. Martins, S. Cardoso, *IEEE Magn. Lett.* **2019**, *10*, 3108605.
22. S. Viveiros, M. Rodrigues, D. Albuquerque, S. A. M. Martins, S. Cardoso, V. C. Martins, *Sensors* **2020**, *20*, 3351.
23. M. J. Camacho, D. C. Albuquerque, E. De Andrade, V. C. Martins, M. L. Inácio, M. Mota, P. P. Freitas, *Sensors* **2023**, *23*, 647.
24. V. C. Martins, J. Germano, F. A. Cardoso, J. Loureiro, S. Cardoso, L. Sousa, M. Piedade, L. P. Fonseca, P. P. Freitas, *J. Magn. Magn. Mater.* **2010**, *322*, 1655.
25. N. R. H. Stone, R. L. Gorton, K. Barker, P. Ramnarain, C. C. Kibbler, *J. Clin. Microbiol.* **2013**, *51*, 1301.
26. S. W. Byun, Y. J. Park, S. Y. Hur, *J. Obstet. Gynaecol.* **2016**, *42*, 422.
27. D.-L. Tang, X. Chen, C.-G. Zhu, Z. Li, Y. Xia, X.-G. Guo, *BMC Infect. Dis.* **2019**, *19*, 798.
28. S. Pudasaini, G. Thapa, B. P. Marasini, B. Giri, *PLOS Glob. Public Health* **2023**, *3*, e0001120.
29. K. R. Healey, C. Jimenez Ortigosa, E. Shor, D. S. Perlin, *Front. Microbiol.* **2016**, *7*, 1995.
30. D. C. Albuquerque, V. C. Martins, E. Fernandes, L. Zé-Zé, M. J. Alves, S. Cardoso, *Biosens. Bioelectron.* **2022**, *210*, 114302.
31. L. M. E. Vanhee, W. Meersseman, K. Lagrou, J. Maertens, H. J. Nelis, T. Coenye, *J. Clin. Microbiol.* **2010**, *48*, 1126.
32. B. B. Fuchs, S. Eatemadpour, J. M. Martel-Foley, S. Stott, M. Toner, E. Mylonakis, *Front. Cell. Infect. Microbiol.* **2019**, *9*, 27.
33. J. Nam, W. S. Jang, D. H. Hong, C. S. Lim, *Sci. Rep.* **2019**, *9*, 3067.
34. V. B. Barbosa, C. F. Rodrigues, L. Cerqueira, J. M. Miranda, N. F. Azevedo, *Front. Bioeng. Biotechnol.* **2022**, *10*, 987669.
35. N. N. Nawar, I. K. Behiry, R. H. A. Yousef, M. A. Emara, *Lab. Med.* **2020**, *51*, 66.

36. S. Scharf, A. Bartels, M. Kondakci, R. Haas, K. Pfeffer, B. Henrich, *Med. Mycol.* **2021**, *59*, 1101.
37. A. Zhu, T. Zembower, C. Qi, *BMC Infect. Dis.* **2021**, *21*, 1159.
38. I. E. Silva, C. Domingues, V. Chu, J. Pedro Conde, *IEEE Sensors J.* **2024**, *24*, 26388.
39. K. Sakai, P. Trabasso, M. L. Moretti, Y. Mikami, K. Kamei, T. Gonoi, *Mycopathologia* **2014**, *178*, 11.
40. P. Pereira-Silva, D. I. Meira, A. Costa-Barbosa, D. Costa, M. S. Rodrigues, J. Borges, A. V. Machado, A. Cavaleiro, P. Sampaio, F. Vaz, *Nanomaterials* **2022**, *12*, 1526.
41. H. Badrane, S. Cheng, C. L. Dupont, B. Hao, E. Driscoll, K. Morder, G. Liu, A. Newbrough, G. Fleres, D. Kaul, J. L. Espinoza, C. J. Clancy, M. H. Nguyen, *Nat. Commun.* **2023**, *14*, 5918.

SUPPORTING INFORMATION

Additional supporting information can be found online in the Supporting Information section at the end of this article.

How to cite this article: M. Zolotareva, F. Cascalheira, R. Afonso, M. Corado, A. Martins, C. Caneiras, C. Bárbara, M. C. Teixeira, D. M. Caetano, *VIEW*. **2025**, *6*, 20250015.
https://doi.org/10.1002/VIW.20250015